Simple Triple-Mode Dual-Polarized Dipole Antenna with Small Frequency Separation Ratio

Jiahao Zhang, Kun Yang, Egil Eide, Sen Yan, and Guy A. E. Vandenbosch

***Abstract*—A triple-mode dual-polarized dipole antenna topology with a very small frequency separation ratio is proposed. The antenna has a simple structure with a very low manufacturing cost, while maintaining a good performance. A conventional dipole is fed by a feeding network also acting as a radiator to generate a second resonant mode. A shorted conductor loaded to the dipole is used to excite a third resonant mode. It is shown that the three modes can be tuned in order to cover different sets of applications. By fusing the two higher resonances, an antenna with a lower band and a very wide higher band can be obtained. Two orthogonal linear polarizations are achieved by integrating two of the aforementioned topologies. The conceptual structure is prototyped and measured. The realized antenna has a lower band of 2.38-2.54 GHz and a higher band of 3.11-4.15 GHz. Its electrical size is 0.8×0.8 λ^2, with a profile of 0.27 λ (λ is the wavelength in free space at 2.4 GHz). The mutual coupling between the two ports is below -20 dB, which is quite beneficial for the diversity performance in MIMO systems.**

***Index Terms*—Multi-band antenna, dual-polarized antenna, dipole antenna, wideband antenna.**

I. Introduction

Nowadays, modern wireless communication systems usually have to combine multiple standards with different working frequencies and protocols [1]. This means that antennas with multiple bands and functions are required. On the other hand, a simple structure and a low cost are also highly desired. Since polarization diversity is a common method to address the issue of multipath fading [2], antennas with dual-polarization are investigated for Multiple Input Multiple Output (MIMO) systems [3]. Considerable efforts have been made to study dual-polarized antennas. [4]-[6] propose wideband dual-polarized antennas to cover various commercial bands simultaneously. However, using a single wideband antenna to cover the separated required bands may introduce unwanted signals in the receiver. In those cases, antennas providing separated bands are superior.

A dual-polarized antenna with two separated bands can be achieved by various topologies, e.g. the microstrip patch antenna [7], [8], the dielectric resonator antenna [9], [10], and the dipole antenna [11], [12]. Normally, researchers have to make a tradeoff between a higher performance, for example more wideband, and a simple structure. Dielectric resonator antennas [9], [10] have a relatively simple topology, but a narrow bandwidth. The microstrip antenna [8] and the dipole antenna [12] achieve a relatively wide bandwidth but with a quite complex structure. The dual-wideband antenna array was also investigated [13], [14]. Again, the topologies of the antenna elements are very complex. Moreover, these dual-band designs have a quite larger frequency separation ratio (2.18 and 2.46 for [13] and [14], respectively). This means that the lower band element and the higher band element can be relatively independently designed, and easily integrated in an array. Note that it is always a challenge to design multi-band antennas with a small frequency separation ratio, suitable for low-frequency wireless communications [15], since the commercial bands at low frequencies are commonly allocated very closely [16], [17]. Compared with dual band operation, triple-band dual-polarized antennas [18], [19] have been relatively less studied. Triple band operation was achieved in [18] with a complicated structure yielding a narrow bandwidth. In [19], the three bands are obtained by three different ports, which increases the complexity.

In this letter, a triple-mode dual-polarized crossed dipole antenna is proposed with a very small frequency separation ratio. The topology is simple with a very low manufacturing cost. Despite its simple structure, the proposed antenna maintains a good performance with a relatively wide bandwidth. It is based on three different resonant working modes. A conventional dipole provides the first resonance. Its feeding network is dimensioned in such a way that it also acts as a radiator to provide the second resonance. A shorted conductor is loaded on the conventional dipole to provide the third resonance. The three resonances are all relatively wideband compared with previous work. Absolutely essential is that the three working modes can be tuned. This yields the potential to achieve different combinations, such as for example three different bands, or a smaller band plus a wide band (the fabricated prototype realizes the latter). All these features make the proposed antenna a good candidate for various applications. The realized antenna has a lower band of 2.38-2.54 GHz, targeting ISM band applications, and a higher band of 3.11-4.15 GHz, targeting WiMAX and WLAN band applications. The mutual coupling between the two ports is below -20 dB, which is quite beneficial for the diversity performance in MIMO systems. Table I gives a comparison of multi-band dual-polarized antennas in literature. The superiority of the proposed antenna is clearly shown. The designed antenna reaches a very small frequency separation ratio and a relatively wide bandwidth with a quite simple topology.

II. Working Mechanism

The design starts from a printed conventional dipole on a substrate (see Ant. 1 in Fig. 1 (a)). The current direction on this conventional dipole is given by the blue arrow. A ground is added to achieve a unidirectional radiation pattern. This dipole is excited by a balun, which in its turn is fed by a feeding line, see Ant. 2 in Fig. 1 (b). A coupling feeding topology is used for the balun, see also [6]. The width of the microstrip feeding line is optimized to achieve good impedance matching for all resonances. The balun structure itself also acts as a grounded dipole antenna, which works at the higher frequency, since its electrical length is shorter than the one of the conventional dipole antenna. In this way, dual band operation is achieved. The current direction on the balun is given by the red arrow. Note that the presence of the ground also invokes a unidirectional radiation pattern for the second resonance. In order to introduce the third resonance, shorting conductors are loaded on the conventional dipole, as shown Fig. 1 (c), Ant. 3. A vertical dipole type current is excited on the shorting conductors, see the green arrows. The radiation pattern of the third

Manuscript received July 7, 2019. This work was supported by the MAMIME project under Grant Agreement No. 256309 by Norwegian Research Council.

J. Zhang and G. A. E. Vandenbosch are with the ESAT-TELEMIC Research Division, Department of Electrical Engineering, KU Leuven, 3001 Leuven, Belgium. K. Yang is with the Super Radio AS, Toftes Gate 2, 0556 Oslo, Norway (e-mail: kun@superradio.no). E. Eide is with the Department of Electronic Systems, NTNU, O.S. Bragstads plass 2b, 7491 Trondheim, Norway. S. Yan is with the Faculty of Electronics and Information, Xi'an Jiaotong University, Xi'an, Shanxi 710049, China.

TABLE I
COMPARISON OF MULTI-BAND DUAL-POLARIZED ANTENNAS IN LITERATURE

Ref.	Freq. band		Tri-band	Freq. separation ratio	Relative complexity		Antenna type
	in GHz	in %					
[7]	1.8 / 5.8	2 / 6.1	No	1:3.22	Low	2 substrates/ 2 connectors/ 1 air layer (supporters)	Microstrip antenna
[8]	0.81-0.96 / 1.69-2.24	16.9 / 28.0	No	1:2.22	High	4 substrates/ 2 connectors/ 2 cables/ 24 metal pins /4 supporters	Microstrip antenna
[9]	1.68-2.02 / 2.34-2.51	18.4 / 7.0	No	1:1.32	Low	1 substrate/ 2 connectors/ 1 metal via/ 1 dielectric block	Dielectric resonant antenna
[10]	1.395 / 2.040	4.3 / 1.2	No	1:1.46	Medium	1 metal ground/ 4 connectors/ 2 baluns/ 4 metal vias/ 1 dielectric block	Dielectric resonant antenna
[11]	2.36-2.76 / 5.12-5.62	15.6 / 9.3	No	1:2.10	Medium	3 substrates/ 2 connectors/ 8 metal pieces	Dipole
[12]	0.80-0.99 / 1.66-2.21	21.2 / 28.4	No	1:2.16	High	1 cavity reflector/ 4 metal plates/ 4 metal blocks/ 4 metal posts/ 4 Γ-probes	Dipole
[18]	0.837-0.848 / 1.425-1.469 / 2.270-2.441	1.3 / 3.0 / 7.3	Yes	1:1.72:2.80	High	2 connectors/ 2 cables/ 1 metal box/ 2 3-dimensional metal structures/ >10 supporters	Cavity slot antenna
This work	2.38-2.54 / 3.11-4.15 (2.45 / 3.2 / 3.8)	6.5 / 28.7	Yes	1:1.31:1.55	Low	3 substrates/ 2 connectors	Dipole

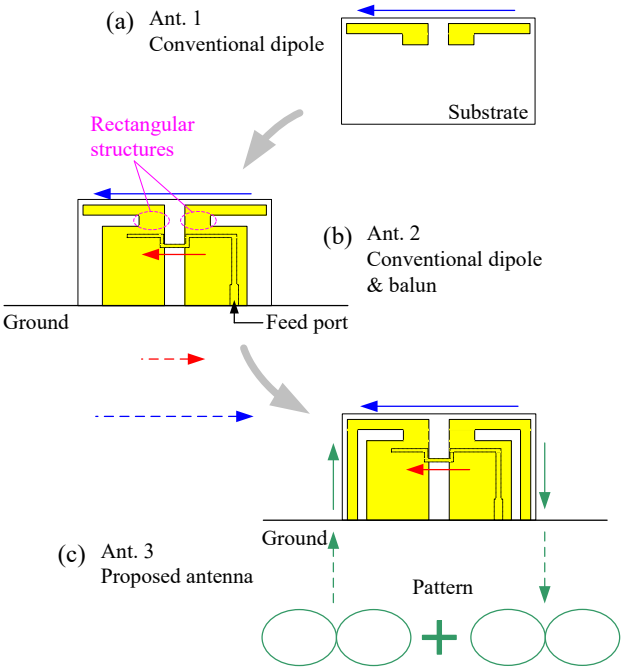


Fig. 1. Design flow of the proposed topology. (a) Initial dipole, (b) Dipole balanced by balun, the feeding line is on the back side of the substrate. (c) Grounding of the dipole ends. The solid arrows indicate the current flow, the dashed arrows indicate the image currents with respect to the ground. The blue arrows describe the current direction of the conventional dipole, the red arrows describe the current direction of the balun, the green arrows describe the current directional of the shorting conductors.

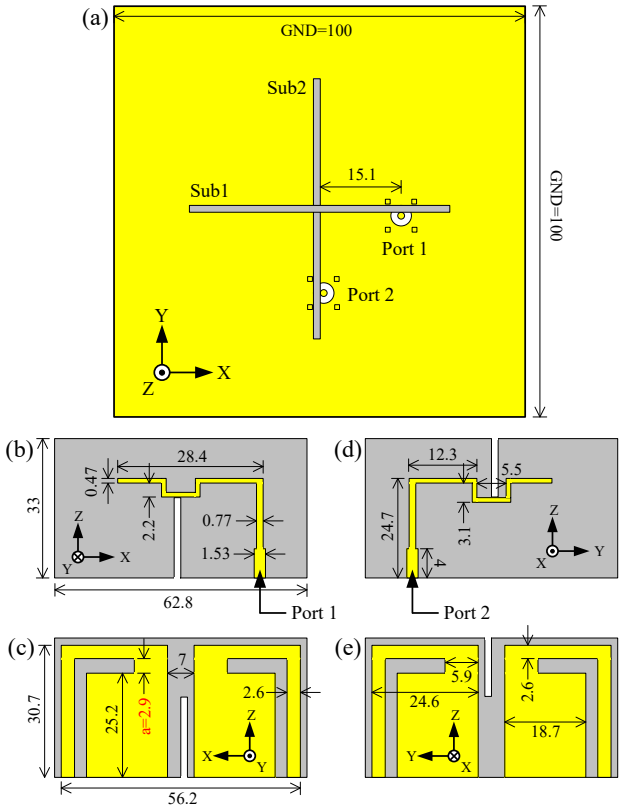


Fig. 2. Topology of the proposed antenna: (a) top view of ground, the slots indicate where the vertical parts are mounted; (b) back of vertical substrate 1: feeding line; (c) front of vertical substrate 1: radiator, (d) back of vertical substrate 2: feeding line, (e) front of vertical substrate 2: radiator. Yellow indicates conductor, gray indicates substrate. Dimensions are in mm.

resonance is the combination of the ones of these two vertical dipoles. Note that rectangular structures (see Fig. 1 (b)) are used between the balun and the conventional dipole to connect them.

These three resonances are mainly excited by the conventional dipole, the shorted conductors, and the balun, respectively. It is crucial to understand that when the resonances are considerably separated in frequency, to a certain extent these three resonances can be tuned separately by tuning the dimensions of these substructures. However, when the resonances come closer together, which is the case we actually study in this paper, the situation is more complex. Further in this paper, the three modes are essentially combined into a narrower lower band (conventional dipole) and a wider higher band (balun + shorted conductor), see also Section III. A single PCB board is used to carry the triple-mode antenna element, in addition to the ground PCB board. The dual polarization is achieved by cross-placing two of such PCB elements on the ground, see details in Section III.

III. DETAILED ANTENNA DESIGN

The detailed topology of the designed antenna is shown in Fig. 2. It contains three 0.8 mm thick FR4 substrates, with permittivity 4.3 and loss tangent 0.025, respectively. Two vertical substrates, which introduce the two orthogonal linear polarizations, are cross-placed on a horizontal ground substrate. The ground is located in the top layer of

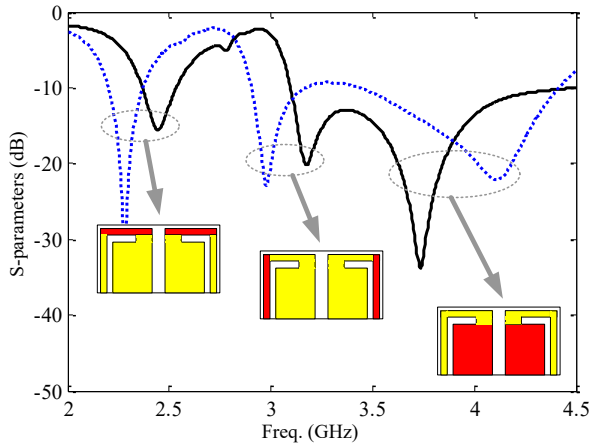


Fig. 3. Simulated reflection coefficient of port 1. The red part indicates the radiating part of the proposed antenna. Black line: dual-band configuration, a=2.9, blue line: triple-band configuration, a=7.0.

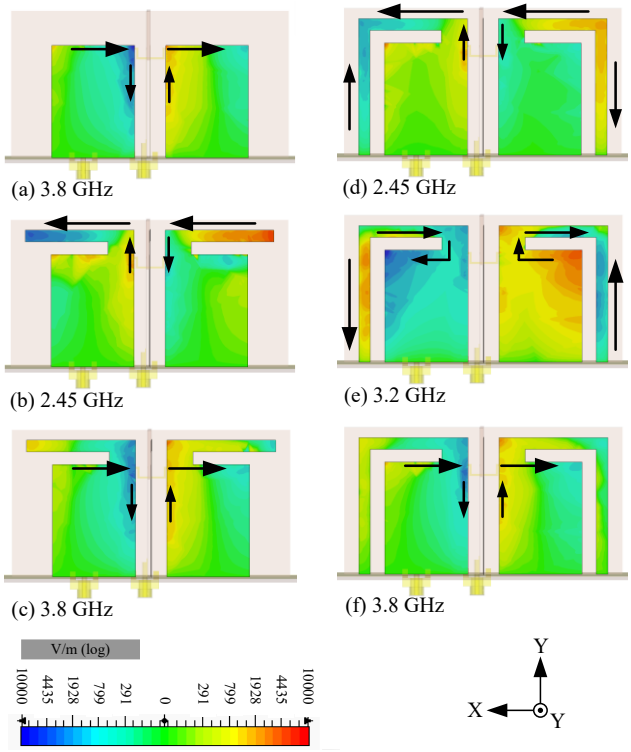


Fig. 5. Y component of E-field distribution. (a) Balun structure at 3.8 GHz. (b) Balun structure + conventional dipole at 2.45 GHz, (c) at 3.8 GHz. (d) Proposed antenna at 2.45 GHz, (e) at 3.2 GHz, (f) at 3.8 GHz. The arrows indicate the simulated current flow.

the ground substrate. The antenna is fed by two straight SMA connectors, whose inner conductors go through the ground substrate to feed a microstrip line on both the vertical substrates, and whose outer conductors are soldered to the ground. Two staggered rectangular slots are cut into the two vertical PCBs, in order to make the crossed mounting on the horizontal ground possible. In this way, a simple, low cost, and stable antenna configuration is achieved. In Fig. 3, as illustration of the flexibility of the topology, the blue line (for a=7 mm) clearly shows three separated resonances, fully covering the 2.305-2.360 GHz wireless communications service bands, the 2.9-3.1 GHz maritime service/ radiolocation service bands, and the 3.7-4.2 GHz next-generation wireless service bands, respectively. For a=2.9 mm (the realized prototype, see next section) these three resonances

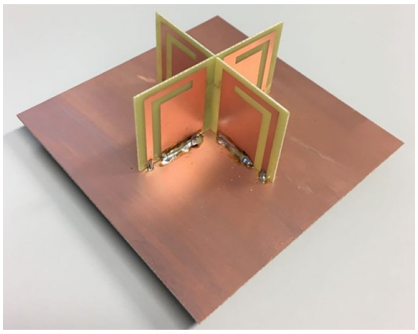


Fig. 4. Prototype of the proposed antenna.

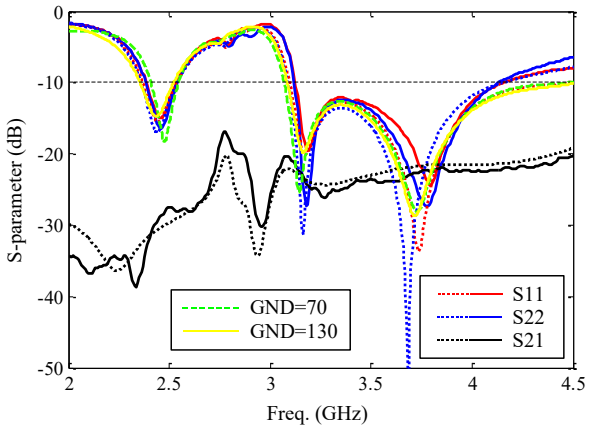


Fig. 6. S-parameters of the proposed antenna. Red lines: reflection at port 1, blue lines: reflection at port 2, black lines: mutual coupling between ports 1 and 2, solid lines: measured results, dashed lines: simulated results. Green line: ground size =70*70 mm^2, yellow line: ground size =130*130 mm^2.

are around 2.45 GHz, 3.2 GHz, and 3.8 GHz. The two upper resonances are fused into one single band. The frequency separation ratios of the three resonances are the smallest ones in literature, only 1:1.31:1.55. The antenna has the potential to cover the 2.4 GHz ISM bands, the 3.5 GHz WiMAX bands, and the 3.6 GHz WLAN bands.

IV. Antenna Performance

A prototype was fabricated, see Fig. 4. For port 1 excited, the simulated y directed component of the electric field (E-field) at 1 mm in y direction away from the metal parts of the antenna is shown in Fig. 5. Fig. 5 (a) indicates the E-field distribution of the balun structure in Ant. 2 at 3.8 GHz. A horizontal current distribution is observed in Fig. 5 (a), which is similar to the current distribution of a dipole. The vertical currents cancel each other. Since a ground is present, a broadside radiation pattern will be observed. Fig. 5 (b) & (c) show the E-field distribution of Ant. 2 at 2.45 GHz and 3.8 GHz, respectively. Fig. 5 (b) shows a typical E-field distribution of a conventional dipole, and Fig. 5 (c) shows a distribution qualitatively similar as in Fig. 5 (a). Fig. 5 (d)-(f) present the E-field distribution of Ant. 3 at 2.45 GHz, 3.2 GHz, and 3.8 GHz, respectively. By loading the shorting conductor, a new resonance at 3.2 GHz is introduced, see Fig. 5 (e). As we can see from this figure, for this middle band resonance, currents are flowing not only on the vertical shorting conductors but also on the conventional dipole part. This means that the pattern of the dipole is combined with the end-fire pattern generated by these two shorting conductors, carrying two opposite currents. Combined with the presence of the ground, this results in a unidirectional broadside radiation pattern with wide beamwidth. Fig. 5 (d) is similar to Fig. 5 (b). The only difference is that a weak current inevitably occurs at the shorting conductor. However, we emphasize that this vertical current

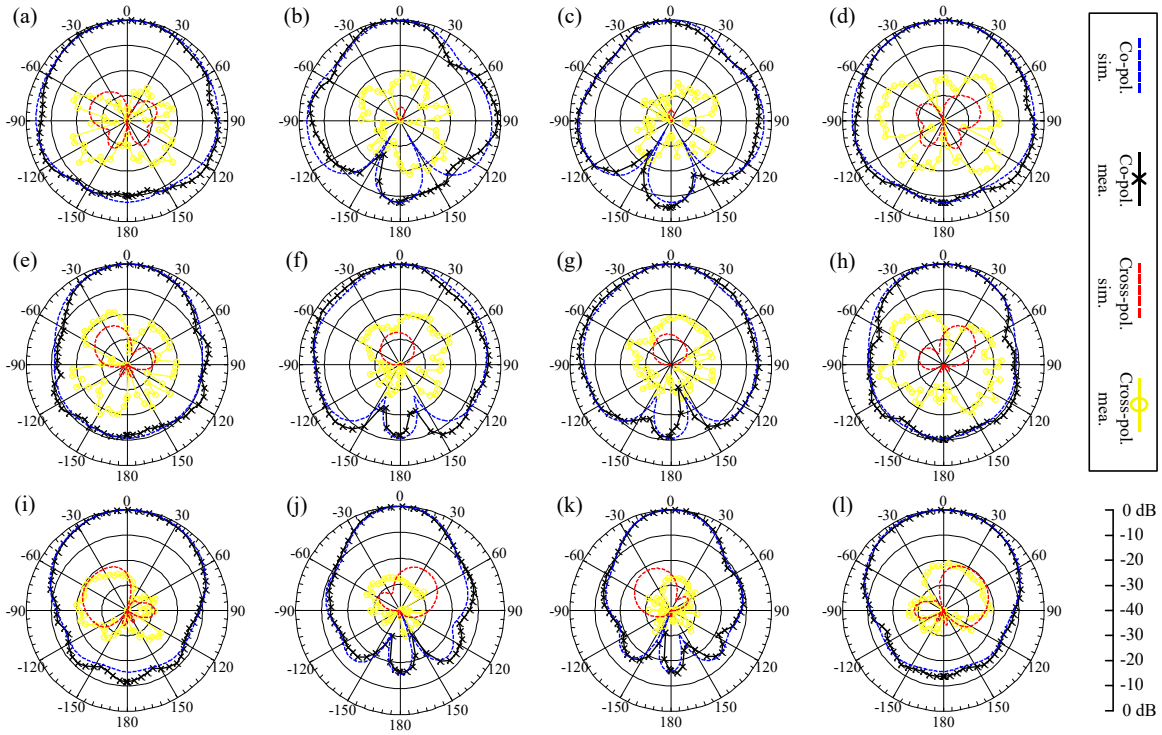


Fig. 7. Normalized radiation patterns. Port 1 at 2.45 GHz (a) XZ plane, (b) YZ plane. Port 2 at 2.45 GHz, (c) XZ plane, (d) YZ plane. Port 1 at 3.2 GHz, (e) XZ plane, (f) YZ plane. Port 2 at 3.2 GHz, (g) XZ plane, (h) YZ plane. Port 1 at 3.8 GHz (i) XZ plane, (j) YZ plane. Port 2 at 3.8 GHz, (k) XZ plane, (l) YZ plane.

TABLE II
REALIZED GAIN AND TOTAL EFFICIENCY

Resonance Freq. (GHz)	Gain (dBi)				Efficiency (%)			
	Mea.		Sim.		Mea.		Sim.	
	P1	P2	P1	P2	P1	P2	P1	P2
2.45	3.7	3.9	3.9	3.8	81	83	85	85
3.2	4.2	4.2	4.2	4.3	79	77	79	79
3.8	6.8	6.6	7.2	7.1	81	78	84	82

does almost not change the resonant frequency, but only widens the beamwidth in E-plane, see also the explanation of Fig. 1 (c). Fig. 5 (f) shows a qualitative similarity with Fig. 5 (a) & (c) at 3.8 GHz.

The S-parameters are given in Fig. 6. Three resonances are clearly seen. The -10 dB lower band is the overlapping band of both port 1 and port 2, realizing the 2.4 GHz ISM band. It is relatively narrow, from 2.38 to 2.54 GHz. The -10 dB higher band is the overlapping band of both port 1 and port 2, realizing the WiMAX and WLAN band. It is a combination of two resonances around 3.2 GHz and 3.8 GHz and is relatively wide: 3.11-4.15 GHz. Note that the ground size is chosen to obtain a tradeoff between a compact size and a relatively high broadside gain. When the size of the ground is changed (see Fig. 6), the resonances will not change much, since the ground mainly acts as reflector. A low mutual coupling between the two ports is observed, below -20 dB in the whole operation band. Fig. 7 presents the measured and simulated normalized radiation patterns. In both the lower and higher bands, unidirectional radiation patterns are observed, with a low cross-polarization level, below -10 dB for all cases. The realized gains and total efficiencies are given in Table II.

In order to investigate the MIMO performance, a 2×2 MIMO array with the proposed antenna element was simulated. The Envelope Correlation Coefficients (ECC) for the most important sets of two co-polarized ports and between the two ports within a single element were calculated based on the simulated far-field patterns [20]. As we can see from Fig. 8, the ECC is below 0.14 in the whole band, which is quite acceptable in MIMO systems.

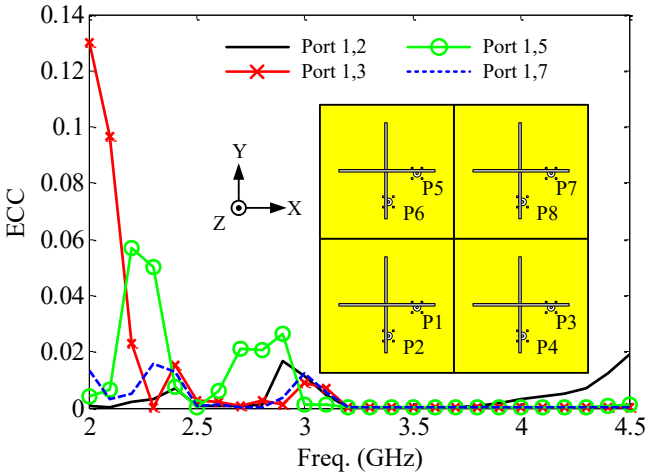


Fig. 8. ECC of a 2×2 MIMO array. Pn indicates port n. Element spacing is 100 mm.

V. CONCLUSION

A novel triple-mode and dual-polarized antenna topology is proposed. Despite its complex functioning, the structure is relatively simple. Three different working modes are combined on a single PCB board. Starting from a conventional dipole, the feeding network of a conventional balun is creatively used to act as a radiation structure to introduce a new resonance. The shorted conductor is also loaded to generate a third resonance. As a concrete example, a prototype has been realized with a narrow lower band and a wide higher band by combining these three working modes, covering 2.38-2.54 GHz in the lower band and 3.11-4.15 GHz in the higher band. A very small frequency separation ratio is thus achieved: 1:1.31:1.55. The antenna has great potential in future MIMO systems.

REFERENCES

[1] J. Zhang, S. Yan, and G. A. E. Vandenbosch, "Metamaterial-inspired dual-band frequency-reconfigurable antenna with pattern diversity," *Electron. Lett.*, vol. 55, no. 10, pp. 573-574, May 2019.

[2] R. G. Vaughan, "Polarization diversity in mobile communications," *IEEE Trans. Veh. Technol.*, vol. 39, no. 3, pp. 177–186, May 1990.

[3] Z. N. Chen and K. M. Luk, *Antennas for Base Station in Wireless Communications.* New York, NY, USA: McGraw-Hill, 2009.

[4] C. Wang, Y. Chen, and S. Yang, S, "Dual-band dual-polarized antenna array with flat-top and sharp cutoff radiation patterns for 2G/3G/LTE cellular bands," *IEEE Trans. Antennas Propag.*, vol. 66, no. 11, pp. 5907-5917, Nov. 2018.

[5] Y. Cui, R. Li, and H. Fu, "A broadband dual-polarized planar antenna for 2G/3G/LTE base stations," *IEEE Trans. Antennas Propag.*, vol. 62, no. 9, 4836-4840, Sep. 2014.

[6] Y. Gou, S. Yang, J. Li, and Z. Nie, "A compact dual-polarized printed dipole antenna with high isolation for wideband base station applications," *IEEE Trans. Antennas Propag.*, vol. 62, no. 8, pp. 4392-4395, Aug. 2014.

[7] D. Y. Lai and F. C. Chen, "A compact dual-band dual-polarized patch antenna for 1800/5800 MHz cellular/WLAN systems," *Microw. Opt. Technol. Lett.*, vol. 49, no. 2, pp. 345–349, Feb. 2007.

[8] Y. Wang and Z. Du, "Dual-polarized dual-band microstrip antenna with similar-shaped radiation pattern," *IEEE Trans. Antennas Propag.*, vol. 63, no. 12, pp. 5923–5928, Dec. 2015.

[9] Y. X. Sun, and K. W. Leung, "Dual-band and wideband dual-polarized cylindrical dielectric resonator antennas," *IEEE Antennas Wireless Propag. Lett.*, vol. 12, pp. 384-387, 2013.

[10] H. Tang, J. X. Chen, W. W. Yang, L. H. Zhou, and W. Li, "Differential dual-band dual-polarized dielectric resonator antenna," *IEEE Trans. Antennas Propag.*, vol. 65, no. 2, pp. 855-860, Feb. 2017.

[11] H. Zhai, K. Zhang, S. Yang, and D. Feng, "A low-profile dual-band dual-polarized antenna with an AMC surface for WLAN applications," *IEEE Antennas Wireless Propag. Lett.*, vol. 16, pp. 2692-2695, 2017.

[12] S. Chen, and K. M. Luk, "High performance dual-band dual-polarized magneto-electric dipole base station antenna," in *2014 Asia-Pacific Microwave Conference (APMC)*, pp. 321-323, Nov. 2014.

[13] Y. He, Z. Pan, X. Cheng, Y. He, J. Qiao, and M. M. Tentzeris, "A novel dual-band, dual-polarized, miniaturized and low-profile base station antenna," *IEEE Trans. Antennas Propag.*, vol. 63, no. 12, pp. 5399-5408, Dec. 2015.

[14] H. Huang, Y. Liu, and S. Gong, "A novel dual-broadband and dual-polarized antenna for 2G/3G/LTE base stations," *IEEE Trans. Antennas Propag.*, vol. 64, no. 9, pp. 4113-4118, Sep. 2016.

[15] J. Zhang, S. Yan, and G. A. E. Vandenbosch, "Realization of dual band pattern diversity with a CRLH-TL inspired reconfigurable metamaterial," *IEEE Trans. Antennas Propag.*, vol. 66, no. 10, pp. 5130-5138, Oct. 2018.

[16] F. J. Herraiz-Martinez, V. Gonzalez-Posadas, L. E. Garcia-Munoz, and D. Segovia-Vargas, "Multifrequency and dual-mode patch antennas partially filled with left-handed structures," *IEEE Trans. Antennas Propag.*, vol. 56, no. 8, pp. 2527–2539, Aug. 2008.

[17] D. Kim, and J. Yeo, "Dual-band long-range passive RFID tag antenna using an AMC ground plane," *IEEE Trans. Antennas Propag.*, vol. 60, no. 6, pp. 2620-2626, Jun. 2012.

[18] Q. Gong, R. L. Li, and Y. Cui, "Tri-band dual-polarised omnidirectional antenna with high isolation for unmanned aerial vehicle applications," *Electron. Lett.*, vol. 54, no. 18, pp. 1059-1060, Sep. 2018.

[19] C. X. Mao, S. Gao, Q. Luo, T. Rommel, and Q. X. Chu, "Low-cost X/Ku/Ka-band dual-polarized array with shared aperture," *IEEE Trans. Antennas Propag.*, vol. 65, no. 7, pp. 3520-3527, 2017.

[20] J. Y. Deng, J. Y.Li, and L. X. Guo, "Decoupling of a three-port MIMO antenna with different impedances using reactively loaded dummy elements," *IEEE Antennas Wireless Propag. Lett.*, vol. 17, no. 3, pp. 430-433, Mar. 2018.